

---

# Climate Data Record (CDR) Program

## Climate Algorithm Theoretical Basis Document (C-ATBD)

### Mean Layer Temperature – UCAR (Lower Stratosphere)



CDR Program Document Number: CDRP-ATBD-0098  
Configuration Item Number: 01B-07  
Revision 3 / June 10, 2015

A controlled copy of this document is maintained in the CDR Program Library.  
Approved for public release. Distribution is unlimited.

**REVISION HISTORY**

<b>Rev.</b>	<b>Author</b>	<b>DSR No.</b>	<b>Description</b>	<b>Date</b>
1	Shu-peng Ben Ho	DSR-488	Initial Submission to CDR Program	08/26/2013
2	Shu-peng Ben Ho	DSR-879	Extension of POR historically	06/10/2015

## TABLE of CONTENTS

<b>1. INTRODUCTION.....</b>	<b>6</b>
1.1 Purpose .....	6
1.2 Definitions.....	6
1.3 Referencing this Document .....	6
1.4 Document Maintenance.....	7
<b>2. OBSERVING SYSTEMS OVERVIEW.....</b>	<b>8</b>
2.1 Products Generated .....	8
2.2 Instrument Characteristics .....	8
<b>3. ALGORITHM DESCRIPTION.....</b>	<b>9</b>
3.1 Algorithm Overview .....	9
3.2 Processing Outline.....	9
3.3 Algorithm Input.....	12
3.3.1 Primary Sensor Data .....	12
3.3.2 Ancillary Data.....	13
3.3.3 Derived Data .....	13
3.3.4 Forward Models.....	14
3.4 Theoretical Description .....	15
3.4.1 Physical and Mathematical Description.....	16
3.4.2 Data Merging Strategy.....	18
3.4.3 Numerical Strategy .....	18
3.4.4 Calculations.....	18
3.4.5 Look-Up Table Description.....	18
3.4.6 Parameterization .....	18
3.4.7 Algorithm Output.....	18
<b>4. TEST DATASETS AND OUTPUTS.....</b>	<b>19</b>
4.1 Test Input Datasets .....	19
4.2 Test Output Analysis .....	21
4.2.1 Reproducibility.....	21
4.2.2 Precision and Accuracy .....	21
4.2.3 Error Budget.....	24
<b>5. PRACTICAL CONSIDERATIONS.....</b>	<b>25</b>
5.1 Numerical Computation Considerations.....	25
5.2 Programming and Procedural Considerations .....	25
5.3 Quality Assessment and Diagnostics .....	25
5.4 Exception Handling .....	28
5.5 Algorithm Validation .....	28
5.6 Processing Environment and Resources .....	32
<b>6. ASSUMPTIONS AND LIMITATIONS .....</b>	<b>33</b>
6.1 Algorithm Performance.....	33

**6.2 Sensor Performance..... 33**

**7. FUTURE ENHANCEMENTS..... 34**

    7.1.1 Enhancement 1 – Revise AQUA Scan Angle Processing.....34

    7.1.2 Enhancement 2 – Improve Algorithm Usage .....34

**8. REFERENCES..... 35**

**APPENDIX A. ACRONYMS AND ABBREVIATIONS..... 37**

## LIST of FIGURES

- Figure 1: Flow chart of processing steps to using GPS RO simulated AMSU TLS (channel 9) to calibrate MSU/AMSU data from multiple MSU/AMSU missions and construct the TLS climate data records. 11
- Figure 2: AMSU Channel 9 Atmospheric weighting functions for a typical atmospheric profile in the Tropics and the Arctic, respectively. The weighting function is defined as  $d(\text{transmittance})/d\ln(p)$ . 13
- Figure 3: Flow chart of the procedures to use RO data to AMSU forward model to compute the simulated AMSU channel 9 Tbs. 15
- Figure 4: The raw AMSU channel 9 Tbs from NOAA 16 reported for November 2002 for (a) the only day of AMSU Tbs with two obviously bad tracks, (b) the monthly mean AMSU channel 9 including all NOAA 16 AMSU Tbs in the same month, and (c) the same as (b), except that it only includes pixels with high quality flags. 20
- Figure 5: Comparison of (a) synthetic CHAMP Tbs and AMSU N18 Ch9 Tbs, (b) COSMIC calibrated N18 AMSU Tbs and CHAMP calibrated N18 AMSU Tbs, (c) synthetic CHAMP Tbs and AMSU N16 Ch9 Tbs, and (d) COSMIC calibrated N16 AMSU Tbs and CHAMP calibrated N16 AMSU Tbs. 24
- Figure 6: The global monthly map in a 2.5 degree x 2.5 degree grid on January 2004 for (a) RO-simulated AMSU TLS, (b) RSS, (c) UAH, and (d) SNO. 26
- Figure 7: The time series of the TLS difference for RSS-RO\_AMSU, UAH-RO\_AMSU, and SNO-RO\_AMSU for (a) the entire globe (82.5°N-82.5°S, the left upper panel), (b) the 82.5°N-60°N zone (the upper right panel), (c) the 60°N-20°N zone (the middle left panel), (d) the 20°N-20°S zone (the middle right panel), (e) the 20°S-60°S zone (the bottom left panel), and (f) the 60°S-82.5°S zone (the bottom right panel). 27
- Figure 8: Comparison of COSMIC-calibrated N15 Tbs and N16-calibrated N15 Tbs. The best fit is in dash line. Diagonal one-to-one fit is in gray solid line. 29
- Figure 9: The time series of the monthly TLS mean differences for TIROS-N6, N6-N7, N7-N8, N8-N9, N10-N11, N11-N12, N12-N14, N14-N15, N16-N15, N19-N18, N14-RO, N15-RO, and Metop-A-N19 for (a) the entire globe (90°N to 90°S), (b) the 90°N to 60°N zone, (c) the 20°N to 60°N zone, (d) the 20°S to 20°N zone, (e) the 60°S to 20°S zone, and (f) the 90°S to 60°S zone. 30
- Figure 10: The time series of the calibrated monthly TLS mean differences for TIROS-N6, N6-N7, N7-N8, N8-N9, N10-N11, N11-N12, N12-N14, N14-N15, N16-N15, N19-N18, N14-RO, N15-RO, and Metop-A-N19 for (a) the entire globe (90°N to 90°S), (b) the 90°N to 60°N zone, (c) the 20°N to 60°N zone, (d) the 20°S to 20°N zone, (e) the 60°S to 20°S zone, and (f) the 90°S to 60°S zone. 31

# 1. Introduction

## 1.1 Purpose

The purpose of this document is to describe the algorithm submitted to the National Centers for Environmental Information (NCEI) by Dr. Shu-peng Ben Ho/COSMIC UCAR. This algorithm produces Advanced Microwave Sounder Unit (AMSU) and Microwave Sounding Unit (MSU) temperatures in the lower stratosphere (TLS, e.g., AMSU channel 9 and MSU channel 4) from National Oceanic and Atmospheric Administration (NOAA), National Aeronautics and Space Administration (NASA), and Europe METeorological Operational satellite-A (Metop/A) satellites which have been calibrated using coincident Global Positioning System (GPS) Radio Occultation (RO) temperature profile measurements from Constellation Observing System for Meteorology, Ionosphere, and Climate (COSMIC) and Challenging Mini-satellite Payload (CHAMP), and Gravity Recovery And Climate Experiment (GRACE) from 2001 to the current. The ‘adjusted’ MSU/AMSU data in the period of 2001 to 2014 will serve as reference data to calibrate other overlapped MSU/AMSU data from 1980 to 2001.

## 1.2 Definitions

Following is a summary of the symbols used to define the algorithm.

Atmospheric parameters:

T = Temperature (1)

P = Pressure (2)

$P_w$  = Vapor Pressure (3)

N = Refractivity (4)

$T_b$  = Brightness Temperature (5)

## 1.3 Referencing this Document

This document should be referenced as follows:

Mean Layer Temperature – UCAR (Lower Stratosphere) - Climate Algorithm Theoretical Basis Document, NOAA Climate Data Record Program CDRP-ATBD-0098 Rev. 3 (2015). Available at <https://www.ncdc.noaa.gov/cdr/fundamental/mean-layer-temperature-ucar-lower-stratosphere>

## **1.4 Document Maintenance**

This document describes the submission, version 2.0, of the processing algorithm and resulting data. The version number will be incremented for any subsequent enhancements or revisions.

## 2. Observing Systems Overview

### 2.1 Products Generated

The objective of this algorithm is to use GPS RO data to serve as climate benchmark to calibrate AMSU/MSU measurements in order to constrain the uncertainties of AMSU-/MSU-inferred TLS trends from 2001 to 2014 and use the ‘adjusted’ MSU/AMSU data in the period of 2001 to 2014 serve as reference data to calibrate other overlapped MSU/AMSU data from 1980 to 2001. Monthly averages over a 34-year period from 1980 through December 2014 from the combined contributions of AMSU/MSU measurements from NOAA, NASA, and MetOp-A polar orbiters are calculated on a 2.5 degree x 2.5 degree grid. The final product consists of monthly mean averages of calibrated AMSU/MSU channel 9 measurements, a mean monthly climatology calculated using 32 full years of data, and monthly anomaly values.

### 2.2 Instrument Characteristics

GPS RO data are highly recommended by the National Science Council (NRC, 2007), the World Meteorological Organization (WMO, 2007), and Global Climate Observing System (GCOS, 2004) as an important component of the global observing system. GPS RO is the only self-calibrated observing technique from space where its fundamental measurement is traceable to the international system of units (SI traceability; Ohring et al., 2007). GPS receivers on low-Earth orbiting (LEO) satellites receive measurable radio frequency signals transmitted from GPS satellites, which, with monitoring and corrections from a series of atomic clocks, allows the GPS time system to be traced to the SI second with a high degree of accuracy. Available GPS RO data from multiple RO missions provide a unique opportunity for monitoring and detecting the vertical structure of atmospheric thermal soundings with high vertical resolution and high accuracy, under all weather conditions.

On board the NOAA series of polar-orbiting satellites, the MSU and the AMSU have also provided near all-weather temperature measurements at different atmospheric vertical layers since 1979 and 1998, respectively. Over the past decade, the roughly 30 years of MSU/AMSU measurements have been extensively used for climate temperature trend detection (Christy et al. 2000, 2003; Mears et al. 2003; Vinnikov and Grody, 2003; Vinnikov et al. 2006; Grody et al. 2004; Zou et al. 2006). Because the MSU/AMSU operational calibration coefficients were obtained from pre-launch datasets (Mo et al. 2001), the orbital changes on MSU/AMSU measurements after launch may not be completely accommodated by these calibration coefficients. Different MSU/AMSU missions may contain different measurement biases, which vary with time and location due to on-orbit heating or cooling of the satellite components. This causes difficulties for climate trend detection (e.g., Christy et al. 2000; Mears et al. 2003; Grody et al. 2004; Zou et al. 2006, 2009).

## 3. Algorithm Description

### 3.1 Algorithm Overview

The processing of calibrated MSU/AMSU data is achieved by the sequential application of programs, which are divided into three logical steps. First, pixel data of radiances for MSU channel 4 and AMSU channel 9 are extracted from the level 1B data sets and stored in daily files for each polar orbiter. In the second step, the MSU channel 4 and AMSU channel 9 brightness temperatures are rebuilt and calibrated by simulated brightness temperatures from GPS RO data. The monthly gridded brightness temperatures are generated. For the final step, the climatology is calculated using 33 years of data. Anomaly values are then obtained by subtracting this climatology from the monthly values. The values are saved in netCDF files.

### 3.2 Processing Outline

The three processing steps are indicated in Figure 1. Input data, indicated by the blue boxes, are acted upon by discrete programs to generate intermediate output files as indicated. In greater detail, these steps which lead to the final output product indicated by the green box are:

**STEP(1) Pre-Processing:** The level 1B data from the polar orbiters are extracted using two IDL (Interface description language) programs. Data from NOAA and METOP orbiters are obtained from the program 'extract\_amsu\_coef.pro' and 'extract\_msu\_coef.pro'. The user must edit this program to specify the name of the polar orbiter, the time interval of data to process, and the input/output paths for the datasets. The programs are then compiled and run separately in IDL for each orbiter. After running these, the extracted values for each orbiter are stored into daily netCDF files for later use.

**STEP(2) Calibration of MSU/AMSU brightness temperatures:** For each GPS mission, channel 9 brightness temperatures ( $T_b$ ) are calculated from vertical profiles of temperature using an AMSU forward model (see Figure 2). The MERRA reanalysis data in HDF format are firstly read and converted to ASCII file by 'merra\_hdf2sav.pro' and 'merra\_sav2txt.pro'. Then the profiles are used to simulate the AMSU channel 9 and MSU channel 4 brightness temperatures for later use. The Modern-ERA Retrospective analysis for Research and Applications (MERRA) reanalysis simulated MSU/AMSU brightness temperatures are used to correct the possible local time drift of the MSU/AMSU measurements.

The set of MSU or AMSU measurements between overlapping NOAA polar orbiters are coincident with these derived values obtained from the IDL program 'match\_noaa\_msuamsu.pro'. The user must edit this program to specify the names of NOAA orbiter, the time interval of data to process, and the tolerances

used to determine coincidence. The program is then compiled and run separately in IDL for each combination of overlapping NOAA orbiters to obtain daily matched measurements. The criteria used to obtain coincident values are 15 minutes in time, 200 km spatial distance, and a scan angle tolerance of 15 degrees. The resulting matched data are stored in daily netCDF files for later use.

Once these datasets are generated for every overlapping polar orbiters, the NOAA14 and NOAA15 are selected as the reference missions to calibrate other MSU and AMSU missions. The offsets are assumed as zero for the reference missions. 11 nonlinear coefficients are assumed for the reference missions. Then simultaneous nadir overpass (SNO) matching data sets are generated from the matched data files by IDL programs 'sno\_step1\_preparematchup\_msu.pro' and 'sno\_step1\_preparematchup\_amsu.pro'. The user must edit the program to specify the matched orbiter names to process. The SNO matchups are used to generate offsets and nonlinear coefficients for other missions by IDL programs 'sno\_step2\_soluteequation\_msu.pro' and 'sno\_step2\_soluteequation\_amsu.pro'. The offsets and nonlinear coefficients are then used to rebuild the brightness temperatures for all the missions by IDL programs 'sno\_step3\_rebuild\_msu.pro' and 'sno\_step3\_rebuild\_amsu.pro'. The user must edit the programs to specify the orbiter name and the time interval of data to process.

Then the MERRA simulated hourly gridded Tbs are used for limb correction and location time correction of MSU and AMSU brightness temperatures. The MSU channel 4 Tbs are converted to AMSU channel 9 Tbs with MERRA simulated data. The Tbs are also binned and saved in netCDF files for later use. These calibration using MERRA are done by 'sno\_step3\_cnadir\_dbin\_msu.pro' and 'sno\_step3\_cnadir\_dbin\_amsu.pro'. The user must edit the program to specify the orbiter name and the time interval of data to process.

The daily zonal mean inter-satellite biases are generated by 'sno\_step4\_intersatbias\_msu.pro' and 'sno\_step4\_intersatbias\_amsu.pro'. The biases between NOAA14 or NOAA15 and GPS-RO are also generated by 'sno\_step4\_satgpsbias.pro'. The user must edit the program to specify the orbiter name to process. Then the modified Christy methods (Christy et al. 2000, 2003) are used to generate the calibration coefficients to remove the inter-satellite biases, seasonal variations, and trends of biases for all the orbiters by IDL programs 'sno\_step5\_christycorr\_msu.pro' and 'sno\_step5\_christycorr\_amsu.pro'. Then the coefficients are used to generate 11 groups of Tbs for all the assumed nonlinear coefficients for reference missions by 'sno\_step6\_christyprod\_msu.pro' and 'sno\_step6\_christyprod\_amsu.pro'. Then the new inter-satellite biases are generated by 'sno\_step7\_new\_intersatbias\_msu.pro' and 'sno\_step7\_new\_intersatbias\_amsu.pro'.

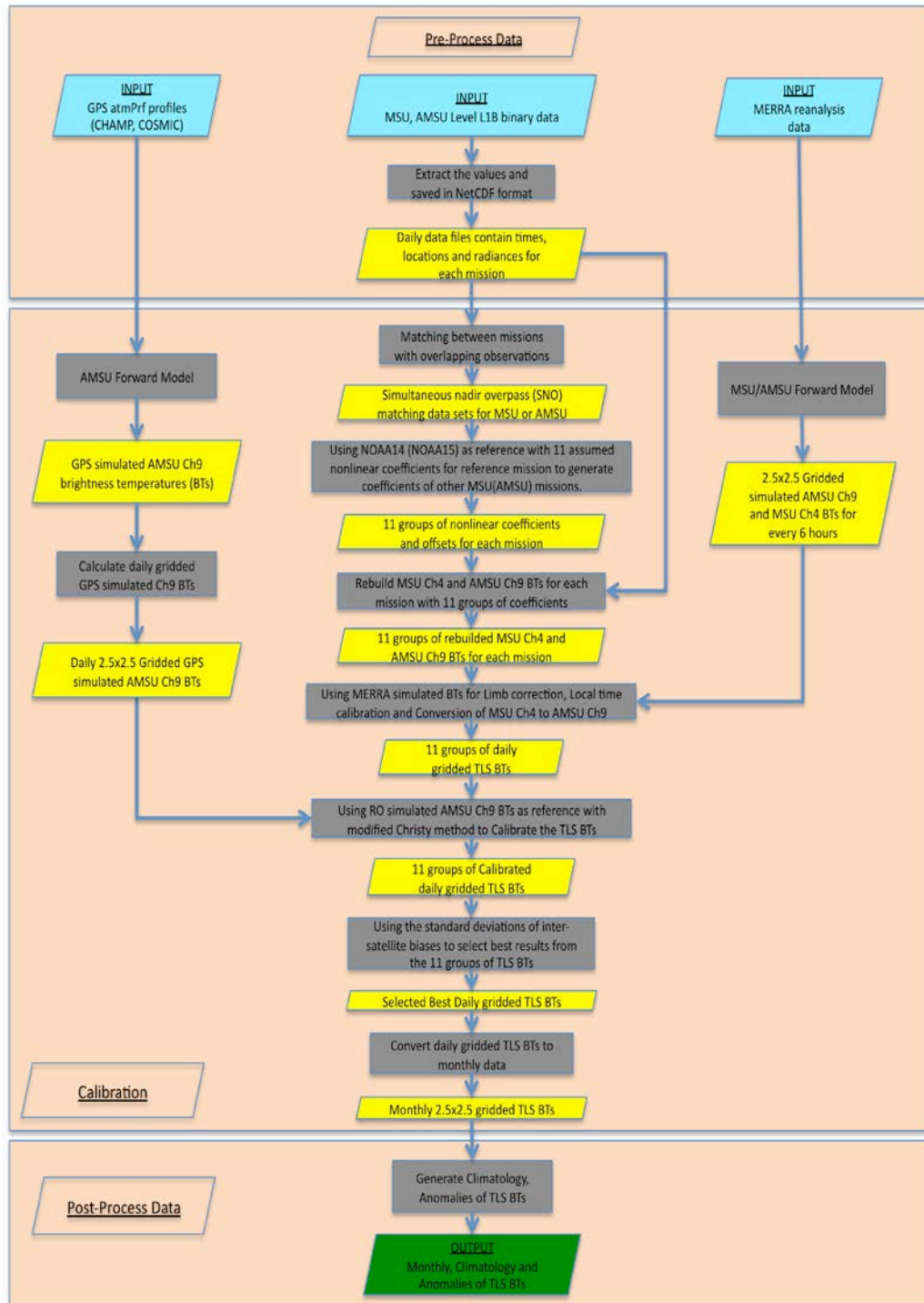


**Figure 1: Flow chart of processing steps to use GPS RO simulated AMSU TLS (channel 9) to calibrate MSU/AMSU data from multiple MSU/AMSU missions and construct the TLS climate data records.**

Then the best results are selected from the 11 groups of the Tbs with the smallest standard deviations of inter-satellite biases by IDL programs 'sno\_step8\_select\_msu.pro' and 'sno\_step8\_select\_amsu.pro'. Then the best results are read and saved in netCDF files by IDL programs 'msu\_daily\_product.pro' and 'amsu\_daily\_product.pro'. Then the daily calibrated results are combined and converted to monthly products by 'monthly\_product.pro'.

**STEP(3) Apply Calibration:** Once all of the monthly gridded values have been generated, the IDL program 'gen\_product.pro' reads in the monthly gridded Tbs, and generates the climatology and anomaly values. The results are written to the final V4 netCDF datasets.

### 3.3 Algorithm Input

#### 3.3.1 Primary Sensor Data

Level 1B AMSU data from NOAA 15, 16, 18, and 19, and from METOP/A, and MSU data from TIROS, NOAA6, 7, 8, 9, 10, 11, 12, 14 are used. For each orbiter, AMSU channel 9 and MSU channel 4 radiance, latitude, longitude, time, and scan angle values are input into the algorithm. The MSU and AMSU level 1B data for NOAA and METOP orbiters are available from the NOAA website <http://www.class.noaa.gov/nsaa/products/welcome>.

From CDACC VERSION 2010.2640 data, dry temperature and water vapor profiles are obtained from ATM and WET data respectively. The profiles from the GPS RO missions COSMIC and CHAMP are first interpolated to 100 pressure levels and then passed to an AMSU forward model to calculate the corresponding channel 9 brightness temperatures. Those derived brightness temperatures, along with latitude, longitude, and time values, are then input into the algorithm. The size of the derived datasets varies with the number of radio occultation events, typically they require about 10 mb per month. All GPSRO profiles were downloaded from the UCAR COSMIC Data Analysis and Archive Center (CDAAC) (<http://cosmic.cosmic.ucar.edu/cdaac/index.html>).

The MERRA reanalysis data are read and interpolated to 100 pressure levels. Then the profiles are passed to AMSU and MSU forward model to calculate the corresponding AMSU channel 9 and MSU channel 4 brightness temperatures. The MERRA data are available in the nasa website (<ftp://goldsmr3.sci.gsfc.nasa.gov:/data/s4pa/MERRA/MAI3CPASM.5.2.0/>)

### 3.3.2 Ancillary Data

N/A

### 3.3.3 Derived Data

The shape and the magnitude of AMSU/MSU temperature weighting function (WF) is a function of the temperature profile (Fig. 2), so using an AMSU/MSU forward model enables one to reduce WF representation errors in the simulated Tbs as compared to those computed from a globally-fixed WF. The forward model  $MWF_{CIMSS}$  from the Cooperative Institute for Meteorological Satellite Studies (CIMSS) was operationally employed in the International ATOVS Processing Package developed at Space Science Engineer Center (SSEC), University of Wisconsin. The validation of microwave transmittance of this model is described in Woolf et al. 1999.

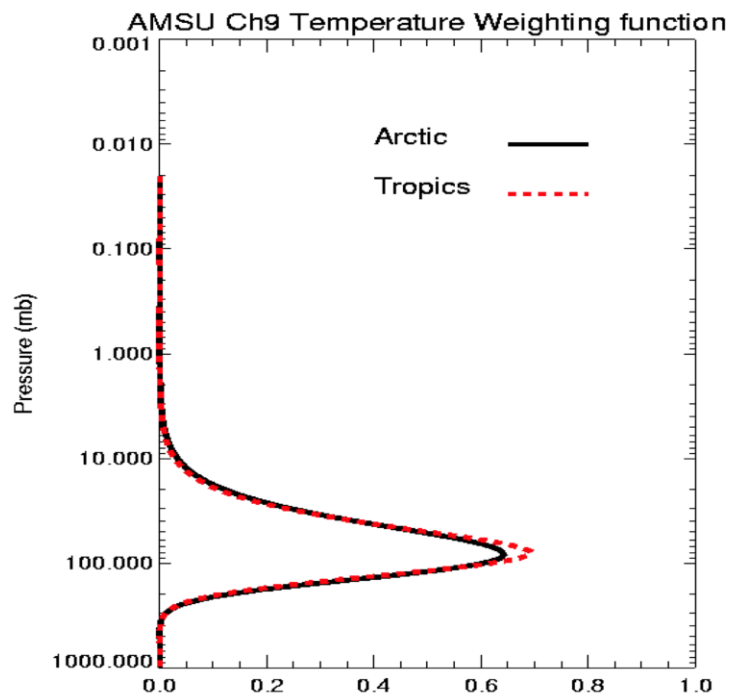


**Figure 2: AMSU Channel 9 Atmospheric weighting functions for a typical atmospheric profile in the Tropics and the Arctic, respectively. The weighting function is defined as  $d(\text{transmittance})/d\ln(p)$ .**

Because the shape and magnitude of AMSU/MSU temperature WF is also a function of viewing geometry, the satellite viewing angle is set to nadir for our calculations.

To perform the conversion of high resolution GPS RO and MERRA temperature profiles into synthetic microwave Tbs, an AMSU/MSU fast forward model with 100 fixed pressure levels from CIMSS (microwave forward model-MWF<sub>CIMSS</sub>) (Hal Woolf, CIMSS, personal communication, 2005) was used. GPS RO soundings and MERRA measurements are interpolated to MWF<sub>CIMSS</sub> levels with reduced vertical resolution.

Instead of using a fixed AMSU9/MSU4 weighting function, we apply each input profile to MWF<sub>CIMSS</sub> to simulate AMSU9/MSU4 Tbs (TLS). This approach ensures that the potential effects of changing TLS weighting functions at various atmospheric temperature structures to calculated Tbs are minimal.

The AMSU or MSU forward model is applied in two steps. First the temperature and water vapor profiles are extracted from the CDACC level2 and MERRA reanalysis data and interpolated to the 100 pressure levels of the forward model and stored into daily data files. Then the forward model is applied to the profiles in each daily file to produce the derived input for the processing algorithm.

In greater detail the steps are:

**STEP(1) Pre-Processing:** The temperature and water vapor data from GPSRO missions are pre-processed using the IDL program 'extract\_gpsro\_profiles.pro'. The user must edit this program to specify the name of the GPSRO mission, the time interval of data to process, and the input/output paths for the datasets. The MERRA reanalysis data are firstly pre-processed using the IDL program 'merra\_hdf2sav.pro' and 'merra\_sav2txt.pro.' The programs is then compiled and run separately in IDL for each mission and MERRA. The extracted profiles for each mission are interpolated to the 100 pressure levels of the AMSU or MSU forward model. After missing values are replaced using seasonal standard atmosphere profiles, the results are stored into daily ASCII files for later use.

**STEP(2) Apply AMSU/MSU Forward Model:** Temperature and water vapor profiles from GPSRO missions and MERRA are then passed to the AMSU/MSU forward model to calculate brightness temperatures for AMSU/MSU channels. The FORTRAN program reads in the profile data for the specified GPSRO mission or MERRA, for the given time interval. The resulting brightness temperature for each day are written to ASCII files for later use as input to the processing algorithm.

### 3.3.4 Forward Models

In this study, CHAMP RO (from 2001 June to 2008 June) and COSMIC (from June 2006 to December 2010) dry temperature profiles are used to compute the synthetic AMSU Ch9 Tbs. The MERRA reanalysis data from 1980 to 2004 are used to generate MSU Ch4 Tbs and data from 2001 to 2014 generate the AMSU Ch9 Tbs. An AMSU fast forward model from the Cooperative Institute for Meteorological Satellite Studies–CIMSS, MWF<sub>CIMSS</sub> (Hal Woolf, CIMSS, personal communication, 2005) is used to project each COSMIC dry temperature profile into synthetic microwave Tbs. The validation of microwave transmittance of this

model is described in Woolf et al. (1999). The Flow chart of the procedures to use RO data to AMSU forward model to compute the simulated AMSU channel 9 Tbs is shown in Fig. 3.

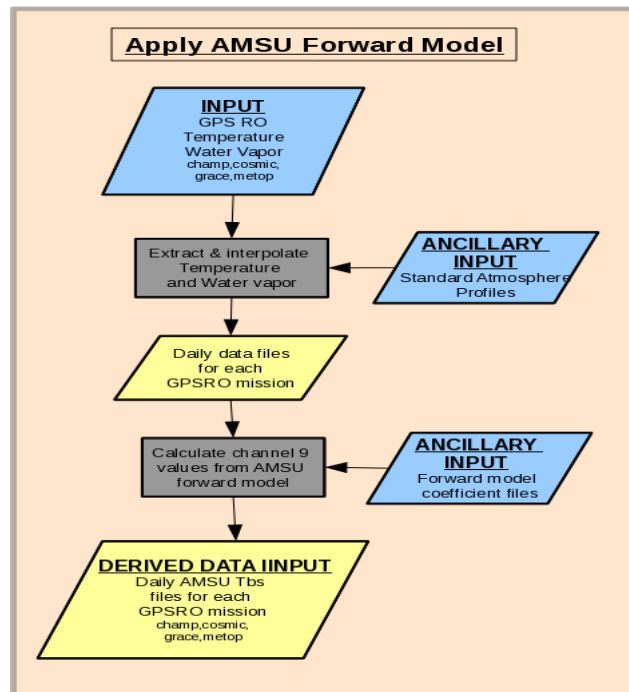


Figure 3: Flow chart of the procedures to use RO data to AMSU forward model to compute the simulated AMSU channel 9 Tbs.

### 3.4 Theoretical Description

The objective of this algorithm is to use GPS RO data to serve as climate benchmark to vicariously calibrate AMSU/MSU measurements and use the 'adjusted' MSU/AMSU data in the period of 2001 to 2014 serve as reference data to calibrate other overlapped MSU/AMSU data from 1980 to 2001. The calibrated and adjusted AMSU/MSU are then used to constrain the uncertainties of satellite-inferred stratospheric and tropospheric temperature trends.

Because the fundamental observable for the GPS RO technique is of high precision and stability that can be traced to the SI unit of second, RO data do not contain mission-dependent biases. This is demonstrated by the collocated soundings of the CHAMP

(launched in 2001) and the COSMIC (launched in 2006) agreeing to within 0.1 K after retrieval (Anthes et al., 2008; Foelsche et al., 2009; Ho et al., 2009a). This makes them potentially useful as a climate benchmark (Ho et al., 2007, 2009c) in addition to being well suited for detecting climate trends (Ho et al., 2009b).

### 3.4.1 Physical and Mathematical Description

Raw RO observations and precise positions and velocities of GPS and LEO satellites, can be used to derive atmospheric refractivity profiles, which are a function of atmospheric temperature and moisture profile (Hajj et al., 2004; Kuo et al., 2004; Ho et al., 2009a). In a neutral atmosphere, the refractivity (N) is related to the pressure (P), the temperature (T) and the partial pressure of water vapor ( $P_w$ ) by the following equation (Bean and Dutton, 1966):

$$N = 77.6 \frac{P}{T} + 3.73 \times 10^5 \frac{P_w}{T^2} \quad (1)$$

The so-called “dry temperature” is obtained by neglecting the water vapor term in equation (1). Above the upper troposphere where moisture is negligible, the dry temperature and the actual temperatures are nearly equal (Ware et al., 1996). In this study the GPS-RO simulated Tbs are used as benchmark to calibrate the MSU and AMSU products.

Firstly an inter-calibration approach using simultaneous nadir overpass (SNO) matchups (Zou et al., 2009) is used to reduce intersatellite biases and warm target temperature contamination. The calibration algorithm as below are used for converting the raw observations (digital counts) to the radiances:

$$R = R_L - \delta R + \mu Z \quad (2)$$

where R is the final earth scene radiance;  $R_L = R_c + S(C_e - C_c)$  representing the dominant linear response and  $S = (R_w - R_c) / (C_w - C_c)$  is the slope;  $Z = S^2(C_e - C_c)(C_e - C_w)$  is a nonlinear response; C represents the raw counts data of the satellite observations; The subscripts e, w and c refer to the earth-view, onboard warm blackbody target view, and cold space view, respectively.  $\delta R$  represents a radiance offset.  $\mu$  is the nonlinear coefficient.

The radiance offset  $\delta R$  and nonlinear coefficient  $\mu$  are assumed to be constant. And the bias of radiance between satellites can be written as:

$$\Delta R_{m,n} = \Delta R_{Lm,n} + (\delta R_m - \mu_m Z) - (\delta R_n - \mu_n Z) \quad (3)$$

The SNO matchups between NOAA missions are used to generate the  $\Delta R_{m,n}$  and  $\Delta R_{Lm,n}$  for all match pairs. The  $\delta R$  for NOAA14 are assumed as 0. So for a given  $\mu$  for NOAA14 the  $\delta R$  and  $\mu$  for NOAA 12 can be generated by solve the equation (3). Then  $\delta R$  and  $\mu$  of NOAA 11 can be obtained with SNO matchups of NOAA12 and NOAA11. The procedure are continued until  $\delta R$  and  $\mu$  for all MSU missions are generated. The  $\delta R$  and  $\mu$  for AMSU missions can also be generated by setting NOAA15 as reference mission. The SNO matchups contain simultaneous observations over the polar region that are less than 2 minutes apart and within 111 km from any NOAA satellite pairs.

The MERRA simulated gridded Tbs are interpolated to the time, location and satellite zenith angle for each MSU measurement ( $T_{MSU}(t, lon, lat, lza)$ ,  $T_{AMSU}(t_0, lon, lat, lza_0)$ ) and AMSU measurement ( $T_{AMSU}(t, lon, lat, lza)$ ,  $T_{AMSU}(t_0, lon, lat, lza_0)$ ). The  $t$ ,  $lon$ ,  $lat$ ,  $lza$  represent the local time, longitude, latitude, satellite zenith angle for the measurement. The MSU channel 4 Tbs are corrected to the local time  $t_0$  and satellite zenith angle  $lza_0$  which are set to 0 and converted to AMSU channel 9 Tbs:

$$T_c = T + T_{AMSU}(t_0, lon, lat, lza_0) - T_{MSU}(t, lon, lat, lza) \quad (4)$$

The AMSU channel 9 Tbs are corrected to the local time  $t_0$  and satellite zenith angle  $lza_0$  which are set to 0:

$$T_c = T + T_{AMSU}(t_0, lon, lat, lza_0) - T_{AMSU}(t, lon, lat, lza) \quad (5)$$

The SNO method can not remove all the biases of Tbs for AMSU or MSU missions. So GPS-RO simulated data are used as 'real' to calibrate the Tbs with modified Christy method. To reduce the seasonal dependent biases of AMSU/MSU Tbs the seasonal bias  $B_{season}$  are introduced in the calibration algorithm. The biases for matched GPS-RO simulated Tbs and NOAA Tbs ( $T_m$ ) can be written as:

$$\Delta T_{ro,m} = bias_{ro,m} - a_m T_{Wm} \quad (6)$$

And biases of Tbs between and NOAA satellites can be written as:

$$\Delta T_{m,n} = bias_{m,n} + a_m T_{Wm} + s_m B_{season} - a_n T_{Wn} - s_n B_{season} \quad (7)$$

Where  $T_w$  is the warm target temperature. In the equation (6), the subscript  $m$  represents NOAA14 for MSU or NOAA15 for AMSU. In the equation (7), the subscripts  $m$  and  $n$  represent from NOAA14 to TIROS or from NOAA15 to METOPA.  $B_{season}$ , which is a function of month, is generated by differences of Tbs between GPS-RO simulated

and NOAA14.  $a$  and  $s$  represent coefficients for warm target and seasonal biases.  $bias_{ro,m}$  and  $bias_{m,n}$  represent the offset for Tbs between NOAA satellites. The equations are solved simultaneously to generate the  $bias_{ro,m}$  and  $bias_{m,n}$ . Then the calibrated Tbs can be written as:

$$\begin{aligned} T_{14c} &= T_{14} - a_{14}T_{W14} - s_{14}B_{season} + bias_{ro,14} \\ T_{12c} &= T_{12} - a_{12}T_{W12} - s_{12}B_{season} + bias_{14,12} + bias_{ro,14} \\ T_{11c} &= T_{11} - a_{11}T_{W11} - s_{11}B_{season} + bias_{12,11} + bias_{14,12} + bias_{ro,14} \end{aligned} \quad (8)$$

Then  $\mu$  for reference mission are selected corresponding the smallest standard deviation of inter-satellite biases for all the missions.

### 3.4.2 Data Merging Strategy

Monthly gridded values for each polar orbiter are calculated by binning and averaging daily gridded data. The combined monthly average for all polar orbiters is calculated by a simple average of the gridded values from each orbiter.

### 3.4.3 Numerical Strategy

N/A

### 3.4.4 Calculations

The calculations primarily consist of binning, averaging, regression of data points.

### 3.4.5 Look-Up Table Description

N/A

### 3.4.6 Parameterization

N/A

### 3.4.7 Algorithm Output

The algorithm results consist of a set of netCDF files, one for each month over the time interval from January 1980 through December 2014. Each file contains the combined calibrated AMSU/MSU mean brightness temperatures (K) from available polar orbiters on a 2.5x2.5 degree grid. Also contained in the file are the number of AMSU observations for each gridpoint, the latitudes and longitudes of gridpoints, and the month, year. Each of the 116 files use less than 100Kb.

## **4. Test Datasets and Outputs**

### **4.1 Test Input Datasets**

#### **a. Quality Control of the AMSU Raw Data**

Before using RO-simulated AMSU channel 9 Tbs to calibrate AMSU Tbs from different satellite missions, we need to ensure only high-quality raw AMSU Tbs are used in the calibration processes. By using quality raw data provided by data processing centers, we are able to identify bad satellite tracks on a specific day for each of the individual satellite missions. This quality control procedure is essential to ensure the quality of the binned monthly mean dataset. For example, if one includes all AMSU channel 9 data without checking the quality flags for each of the individual satellite pixels, some obvious bad data from certain tracks (for example, Fig. 4a) will be included in the binning procedures and the binned monthly mean TLS will be highly contaminated (Fig. 4b). The monthly mean TLS, including only AMSU data with good quality flags, is shown in Fig. 4c.

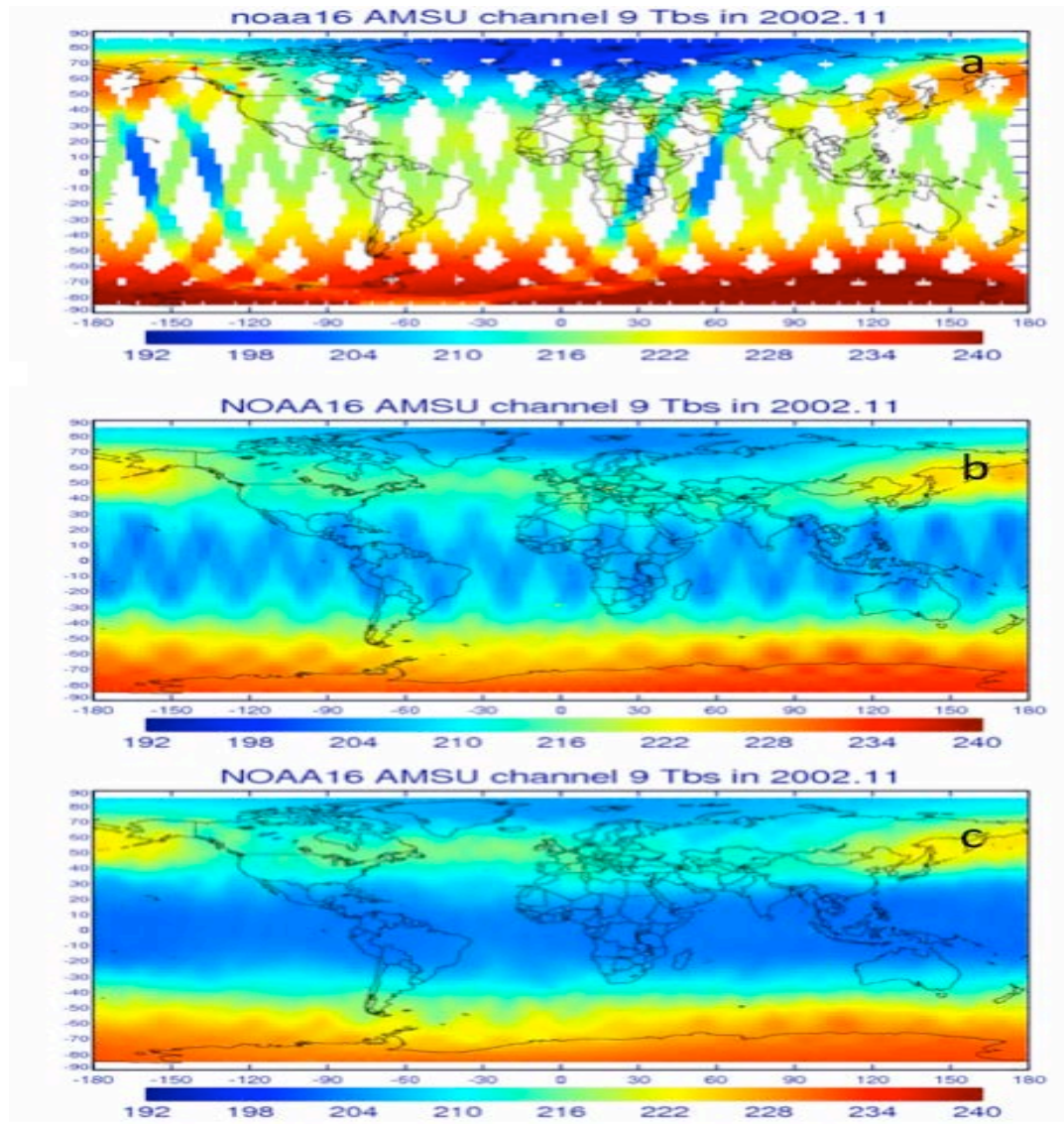


Figure 4.: The raw AMSU channel 9 Tbs from NOAA 16 reported for November 2002 for (a) the only day of AMSU Tbs with two obviously bad tracks, (b) the monthly mean AMSU channel 9 including all NOAA 16 AMSU Tbs in the same month, and (c) the same as (b), except that it only includes pixels with high quality flags.

## b. Two Months of Test Data

Two months of test data from November and December of 2006 are provided with the IDL and FORTRAN source programs. The directory [\\$SRC/Test-Data/Input/AMSU/](#) contains sub-directories containing L1B polar orbiter data for NOAA-15, NOAA-16,

NOAA-18, and AQUA. The directory *\$SRC/Test-Data/ASCII tmp/gps AMSU Tbs/* contains the derived AMSU brightness temperatures from the COSMIC and CHAMP GPSRO missions. These are the input data used by the processing algorithm. The other directories; *extract/*, *match/*, *offset slope/*, and *bin/* in the *\$SRC/ASCII tmp/* directory contain the intermediate processing results from each IDL program for these two months. The final netCDF results are contained in the *\$SRC/Test-Data/Output/* directory.

## **4.2 Test Output Analysis**

### **4.2.1 Reproducibility**

Along with the two months of level 1B AMSU data and GPS RO derived brightness temperatures, all of the intermediate datasets generated during processing leading up to the final results are provided. Applying the processing algorithm to the input datasets, the user should recover exact results for each of these intermediate files. Differences in any of these intermediate or final results are indicative of an error.

### **4.2.2 Precision and Accuracy**

#### **a. Precision and Accuracy of RO Data**

Kuo et al. (2004) showed that GPS RO soundings have very high accuracy (up to 0.3% in terms of refractivity) in the layer between 5 to 25 km. Ho et al., (2009a) showed that collocated CHAMP and COSMIC dry temperature differences between 500 hPa and 10 hPa range from -0.35 K (at 10 hPa) to 0.25 K (at 30 hPa) and their mean difference is about -0.034 K. The fact that the mean dry temperature difference in the height ranging from 500 hPa to 10 hPa is within the normalized standard error of the mean difference demonstrates long-term stability of the GPS RO signals. Since the AMSU forward model cannot introduce additional variability, the precision of these temperature measurements at altitudes sensitive to AMSU channel 9 results in stable reference values for channel 9 brightness temperatures.

To quantify the accuracy of RO temperature profile, we compared RO temperature profiles collocated with high quality radiosonde data. Temperature comparison between COSMIC and temperature measurements from Vaisala-RS92 show that COSMIC temperature is very close to those of radiosondes from 200 hPa to 20 hPa (around 12 km to 25 km) with a zero mean (He et al., 2009; Ho et al., 2010a).

#### **b. Precision and Accuracy of RO Derived AMSU TLS**

We also quantify the accuracy of the defined slope and offset by finding the difference between COSMIC calibrated N18 AMSU Tbs ( $T_{b_{\text{COSMIC\_N18}}}$ ) and CHAMP calibrated N18 AMSU Tbs ( $T_{b_{\text{CHAMP\_N18}}}$ ); the  $T_{b_{\text{CHAMP\_N18}}}$  was found by comparing synthetic CHAMP

Tbs ( $T_{b_{CHAMP}}$ ) to the collocated  $T_{b_{AMSU\_N18}}$  using the procedures introduced in Section 3. Again, CHAMP, COSMIC, N16 and N18 AMSU data from Sep. 2006 are used. The scatter plot for the CHAMP-N18  $T_b$  comparison is shown in Fig. 5a and the slope and offset of the CHAMP-N18 pairs is defined. The  $T_{b_{CHAMP\_N18}}$  and  $T_{b_{COSMIC\_N18}}$  can be then computed using the following equations when N18  $T_b$ s from CHAMP-N18 pairs are used as inputs:

$$T_{b_{CHAMP\_N18}} = 0.973 \times T_{b_{AMSU\_N18}} + 6.90 \quad (2)$$

$$T_{b_{COSMIC\_N18}} = 0.96 \times T_{b_{AMSU\_N18}} + 8.68. \quad (3)$$

The slope and offset defined in Eq. (3) are found using COSMIC-N18 pairs. Then we apply the same N18  $T_b$ s from CHAMP-N18 pairs to Eqs. (2) and (3) to find  $T_{b_{COSMIC\_N18}}$  and  $T_{b_{CHAMP\_N18}}$ . Therefore, by finding the difference between  $T_{b_{COSMIC\_N18}}$  and  $T_{b_{CHAMP\_N18}}$ , we can determine if the slope and offset in Eq. (3) are still valid when different N18  $T_b$ s are used as inputs. The scatter plot of  $T_{b_{COSMIC\_N18}}$  and  $T_{b_{CHAMP\_N18}}$  is shown in Fig. 5b. The correlation coefficient of  $T_{b_{CHAMP\_N18}}$  and  $T_{b_{COSMIC\_N18}}$  is equal to 1.0 and the mean bias between  $T_{b_{COSMIC\_N18}}$  and  $T_{b_{CHAMP\_N18}}$  is very close to zero ( $\sim 0.07$  K). The very tight fit of  $T_{b_{COSMIC\_N18}}$  and  $T_{b_{CHAMP\_N18}}$  (the standard deviation is about 0.1 K) demonstrates the consistency between the slope and offset (calibration coefficients) found in the N18-CHAMP pairs and that from N18-COSMIC pairs.

To see if we can find a similar conclusion for the GPS RO calibrated AMSU  $T_b$ s from other NOAA satellites, we repeat the above procedures but replace  $T_{b_{AMSU\_N18}}$  with  $T_{b_{AMSU\_N16}}$ , where COSMIC calibrated N16 AMSU  $T_b$ s ( $T_{b_{COSMIC\_N16}}$ ) and CHAMP calibrated N16 AMSU  $T_b$ s ( $T_{b_{CHAMP\_N16}}$ ) can be computed using the following equations when the same N16  $T_b$ s from CHAMP-N16 pairs are used as inputs:

$$T_{b_{CHAMP\_N16}} = 0.984 \times T_{b_{AMSU\_N16}} + 4.05 \quad (4)$$

and

$$T_{b_{COSMIC\_N16}} = 0.978 \times T_{b_{AMSU\_N16}} + 5.50. \quad (5)$$

The scatter plots similar to Figs. 5a and 5b are shown in Figs. 5c and 5d, respectively. It is shown in Fig. 5c that we have fewer N16-CHAMP pairs when compared to that of N18-CHAMP pairs (Fig. 5a). This is because the distribution of CHAMP data is more synchronized to that of N18 than that of N16 in this month. The fact that the mean difference ( $-0.07$  K) and standard deviation ( $\sim 0.1$  K) between  $T_{b_{COSMIC\_N16}}$  and  $T_{b_{CHAMP\_N16}}$  is compatible to those from  $T_{b_{COSMIC\_N18}}$  and  $T_{b_{CHAMP\_N18}}$  demonstrates that even with fewer samples (from CHAMP-N16 pairs in this month), because of the high precision of GPS RO data, we can still define robust slopes and offsets for NOAA-CHAMP pairs which are consistent with those derived from NOAA-COSMIC pairs.

Results in Figs. 5b and 5d can also be interpreted as an indirect estimate of the precision of the averaged  $T_{b_{\text{COSMIC}}}$  and  $T_{b_{\text{CHAMP}}}$  where N18/N16 Tbs are used as cross references, although different N18/N16 samples are used for N18/N16-CHAMP and N18/N16-COSMIC pairs. This indicates that, even though we cannot directly compare  $T_{b_{\text{COSMIC}}}$  and  $T_{b_{\text{CHAMP}}}$ , by comparing  $T_{b_{\text{COSMIC\_AMSU}}}$  and  $T_{b_{\text{CHAMP\_AMSU}}}$ , where slopes and offsets from N18-COSMIC and N18-CHAMP pairs respectively are used, we can still define the precision between  $T_{b_{\text{COSMIC}}}$  and  $T_{b_{\text{CHAMP}}}$ . The  $\pm 0.07$  K mean differences of GPS RO-NOAA pairs and  $\sim 0.1$  K of standard deviation may still be related to the natural variability within 50 km separation distance and 30-minute time difference. In the future, more samples with a smaller time difference and separation distance will be used to provide better estimation of the mean difference and precision between  $T_{b_{\text{COSMIC}}}$  and  $T_{b_{\text{CHAMP}}}$ . A smaller mean bias and a higher precision between  $T_{b_{\text{COSMIC}}}$  and  $T_{b_{\text{CHAMP}}}$  can be expected.

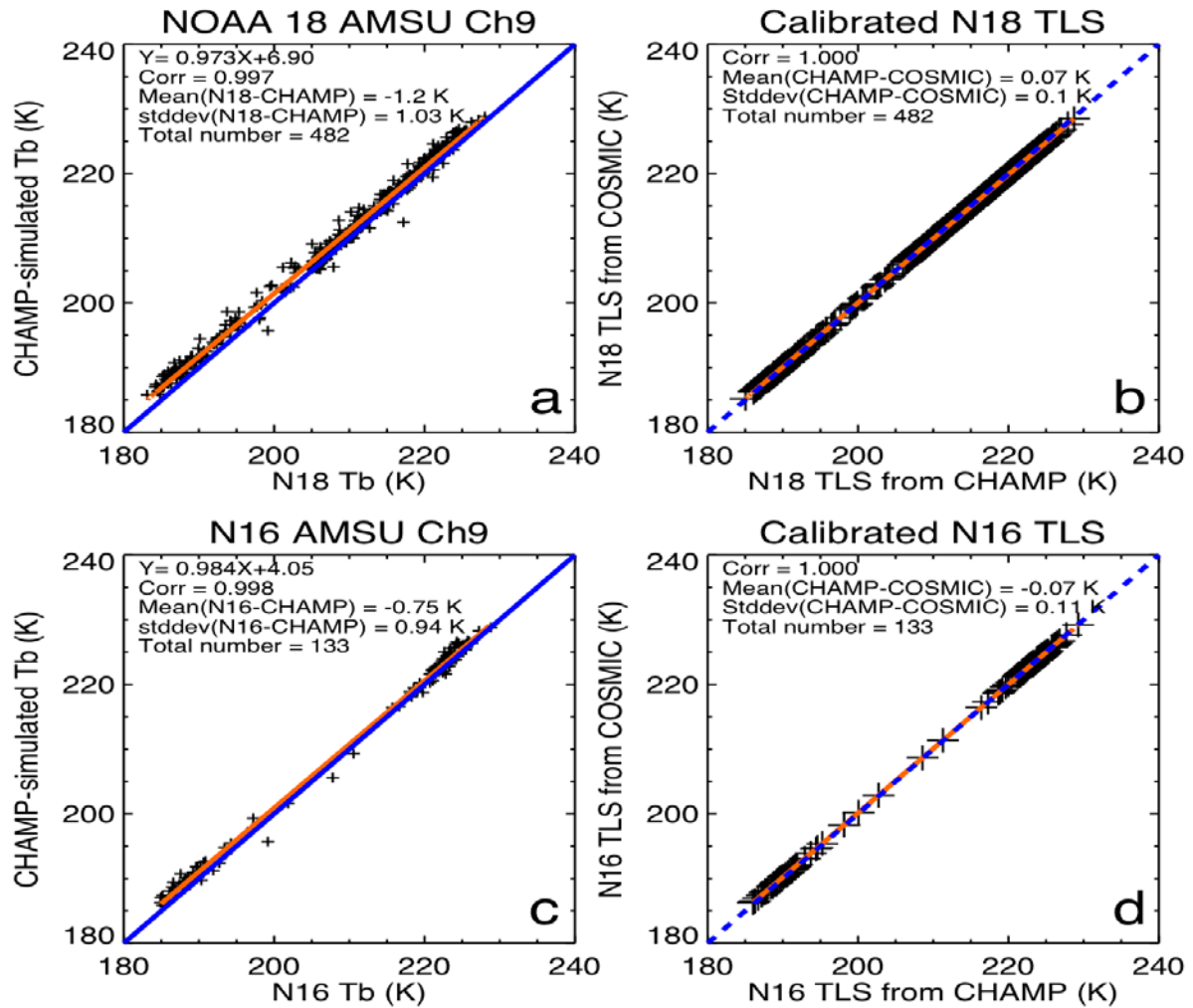


Figure 5: Comparison of (a) synthetic CHAMP Tbs and AMSU N18 Ch9 Tbs, (b) COSMIC calibrated N18 AMSU Tbs and CHAMP calibrated N18 AMSU Tbs, (c) synthetic CHAMP Tbs and AMSU N16 Ch9 Tbs, and (d) COSMIC calibrated N16 AMSU Tbs and CHAMP calibrated N16 AMSU Tbs.

### 4.2.3 Error Budget

N/A

## 5. Practical Considerations

### 5.1 Numerical Computation Considerations

IDL is not well suited to take full advantage of SMP environments. Since the computationally intense programs typically have to be run separately for each RO mission or polar orbiter, processing is optimized by simultaneously running separate IDL sessions.

### 5.2 Programming and Procedural Considerations

Execution of the IDL programs requires that the user edit the program file to specify the run parameters controlling execution. Programs must then be compiled and run from within an IDL session.

### 5.3 Quality Assessment and Diagnostics

To assess the quality of the derived TLS record, we compare the derived TLS record with other TLS datasets. Here we briefly introduce comparison results using the derived TLS record with the newly available TLS datasets provided by RSS (Remote Sensing System Inc.) and UAH (University of Alabama in Huntsville), and TLS processed by NOAA Center for Satellite Applications and Research (STAR, using simultaneous nadir overpass-SNO method) from 2001 to 2010. This is to demonstrate the quality of the derived TLS record.

#### a. Global Monthly Maps of RSS, UAH, STAR, and RO\_AMSU TLS

**Figure 6** shows the global monthly mean map in a 2.5 degree x 2.5 degree grid on January 2004 for RSS, UAH, SNO, and RO-simulated AMSU TLS.

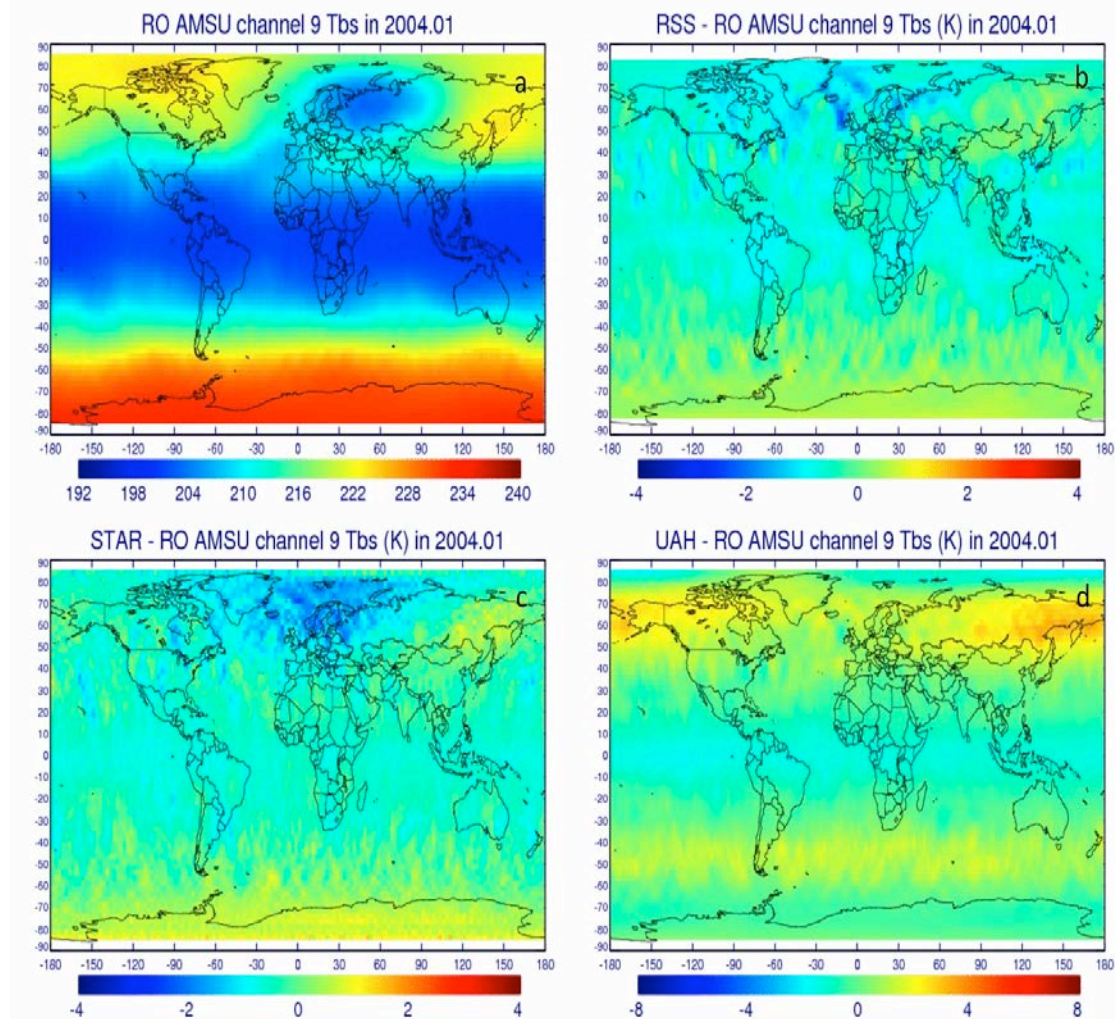


Figure 6: The global monthly map in a 2.5 degree x 2.5 degree grid on January 2004 for (a) RO-simulated AMSU TLS, (b) RSS, (c) UAH, and (d) SNO.

## b. Time Series of RSS, UAH, STAR, and RO\_AMSU TLS Anomalies

Figure 7 shows that the time series of the TLS difference among RSS, UAH, and SNO relative to that of RO\_AMSU vary with different latitudinal zones. The TLS anomalies from SNO generally agree well with those from RO-calibrated AMSU TLS in all latitudinal zones.

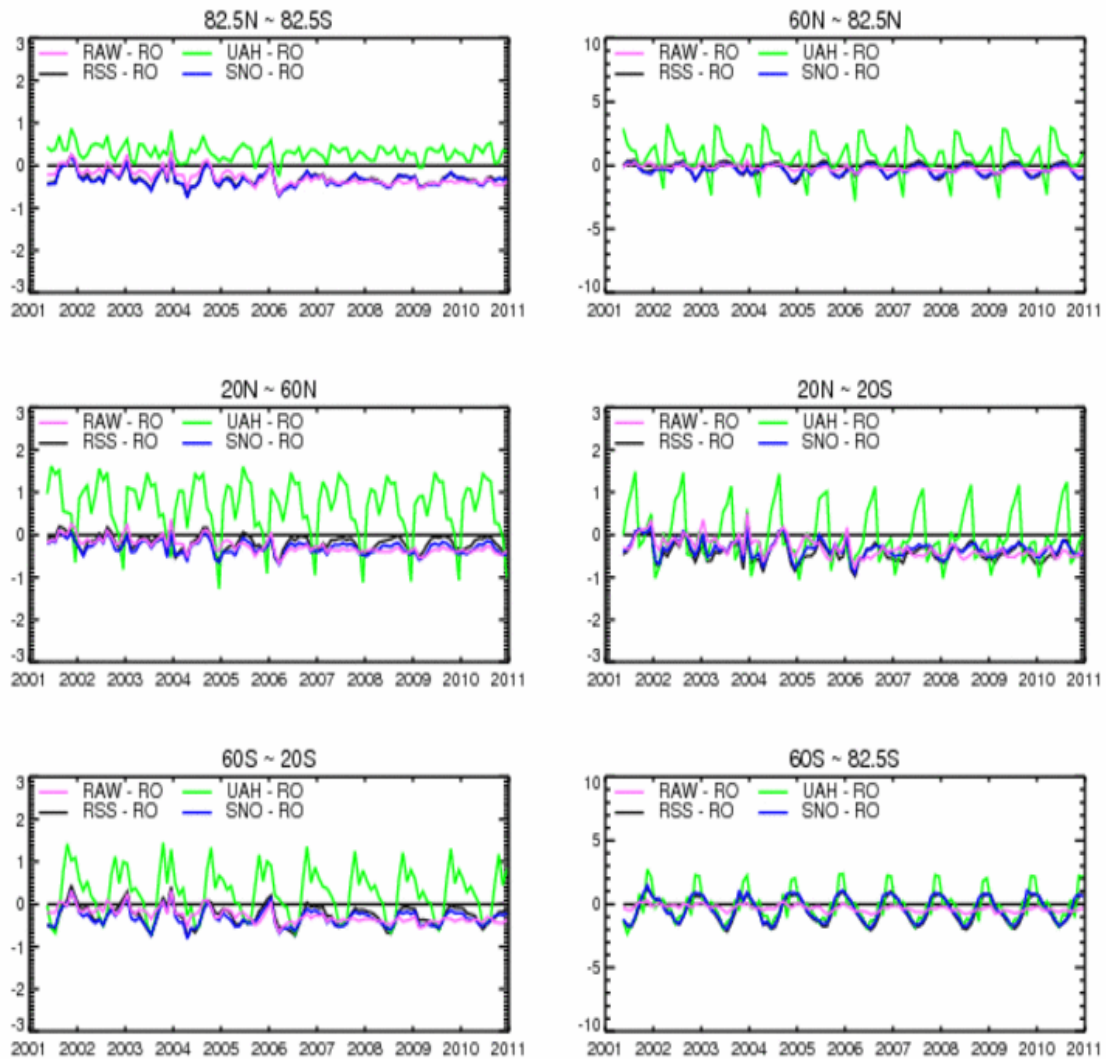


Figure 7: The time series of the TLS difference for RSS-RO\_AMSU, UAH-RO\_AMSU, and SNO-RO\_AMSU for (a) the entire globe (82.5°N-82.5°S, the left upper panel), (b) the 82.5°N-60°N zone (the upper right panel), (c) the 60°N-20°N zone (the middle left panel), (d) the 20°N-20°S zone (the middle right panel), (e) the 20°S-60°S zone (the bottom left panel), and (f) the 60°S-82.5°S zone (the bottom right panel).

## 5.4 Exception Handling

The program will stop and print out an informative message for all *known* error conditions.

## 5.5 Algorithm Validation

To further validate the calibration algorithm, we perform extra tests using RO and AMSU data as the following. Here we used a similar calibration method in this test study. RO simulated AMSU Tbs are used to further inter-calibrate the pixel level microwave Tbs (NESDIS<sub>OPR</sub>) from 2009 to 2012, and validate new available NEN<sub>NEW</sub> after 2006 according to the availability of the data. The calibrated MSU/AMSU TLS will be served as reference data to calibrate other overlapped MSU/AMSU data. Recently Ho et al., (2008b) has demonstrated the feasibility of this approach by examining whether the calibration coefficients (slope and offset) found from NOAA 15 (N15)- NOAA 16 (N16) pairs and N16-COSMIC pairs are consistent to that constructed from COSMIC-N15 pairs. This is to see if we have only N16-COSMIC pairs and N15-N16 pairs, how consistent is the constructed N15 Tbs (denoted as N16-calibrated N15 Tbs) and COSMIC-calibrated N15 Tbs. Figure 8 shows the comparison of COSMIC-calibrated N15 Tbs and N16-calibrated N15 Tbs. The very tight fit of the COSMIC-calibrated N15 Tbs and N16-calibrated N15 Tbs (with mean bias ~ 0.06K and standard deviation ~ 0.04 K) show that the calibration coefficients found from NOAA-NOAA pairs are also consistent with that of NOAA-COSMIC pairs. This gives us confidence in using the RO-calibrated MSU/AMSU Tbs to calibrate other overlapped MSU/AMSU Tbs when RO data are not available.

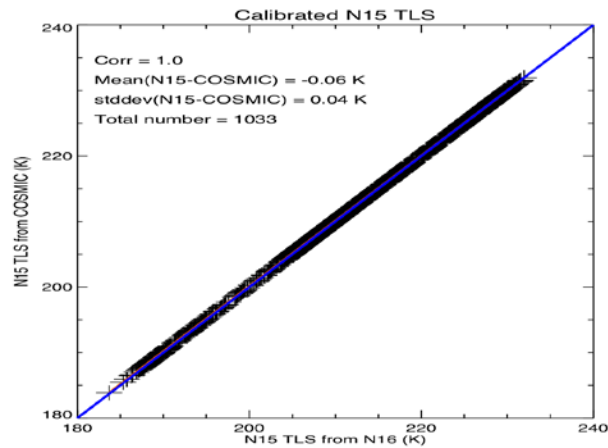


**Figure 8: Comparison of COSMIC-calibrated N15 Tbs and N16-calibrated N15 Tbs. The best fit is in dash line. Diagonal one-to-one fit is in gray solid line.**

The recommended approach to further validate the program will be to use RO data from multiple RO missions after 2010 to simulate AMSU Tbs and use the simulated AMSU Tbs to further inter-calibrate the pixel level microwave Tbs (NESDIS<sub>OPR</sub>) from multiple AMSU mission and inter-compare the consistency between the calibrated Tbs as above.

We used those AMSU and MSU TLS calibrated by multiple RO missions from 2001 to 2013 to calibrate those overlapped AMSU and MSU TLS form 1978 to 2001. Figure 9 depicts the inter-satellite biases between two missions when they are co-located. The inter-satellite biases between TIROS-N6, N6-N7, N7-N8, N8-N9, N10-N11, N11-N12, N12-N14, N14-N15, N16-N15, N19-N18, N14-RO, N15-RO, and Metop-A-N19 are generated.

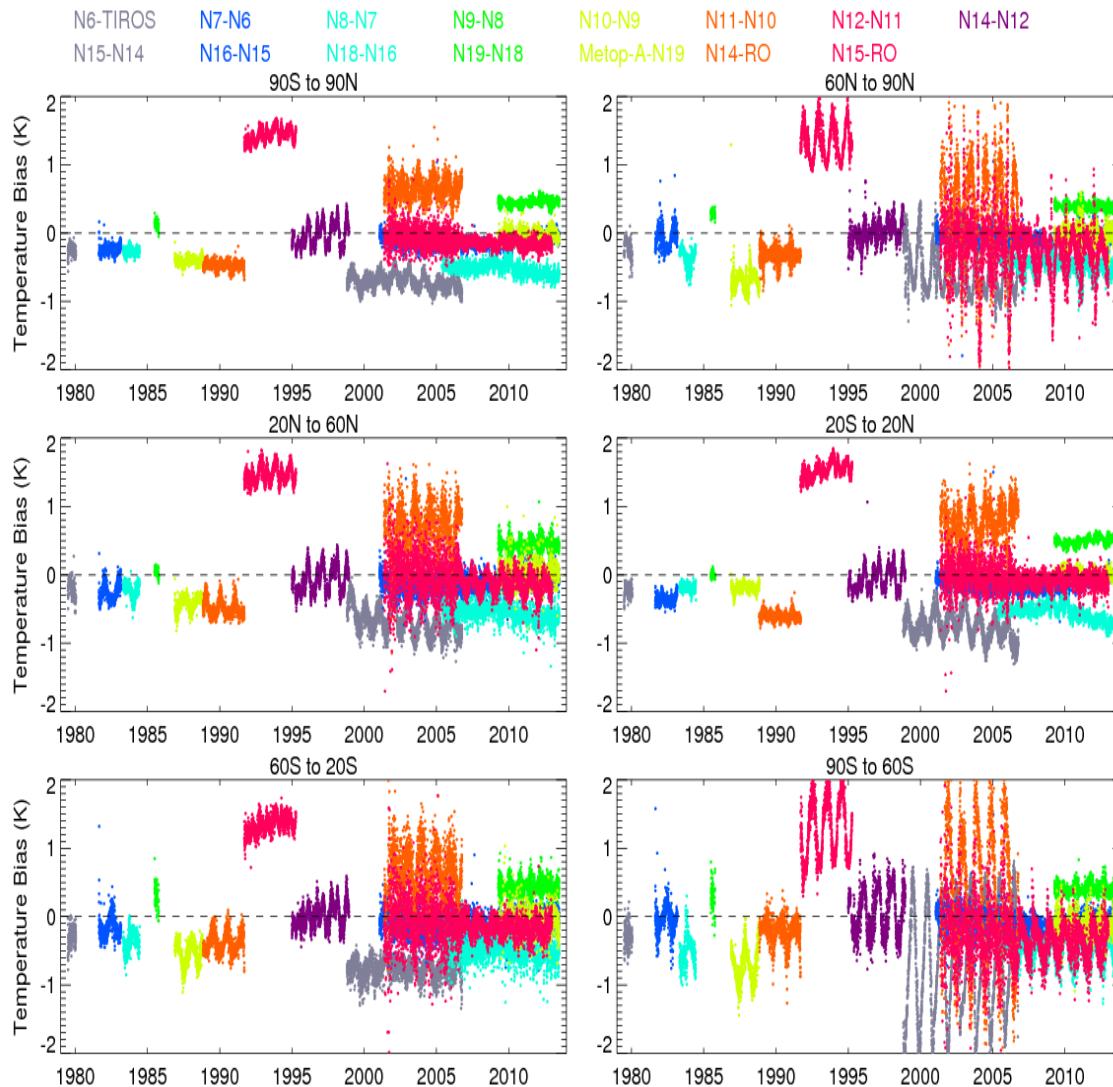


**Figure 9: The time series of the monthly TLS mean differences for TIROS-N6, N6-N7, N7-N8, N8-N9, N10-N11, N11-N12, N12-N14, N14-N15, N16-N15, N19-N18, N14-RO, N15-RO, and Metop-A-N19 for (a) the entire globe (90°N to 90°S), (b) the 90°N to 60°N zone, (c) the 20°N to 60°N zone, (d) the 20°S to 20°N zone, (e) the 60°S to 20°S zone, and (f) the 90°S to 60°S zone.**

Applying the RO calibrated MSU NOAA 14 data as references to calibrate overlapped NOAA 12 MSU and repeating the procedures, we were able to calibrate MSU data before 2001 and construct consistent AMSU/MSU TLS climate data records from 1980 to 2013. The calibrated TLS from 1980 to 2013 is shown in Figure 10. The results show that the calibrated AMSU/MSU TLS between two overlapped NOAA or RO missions are all very close to zero degree K no matter they are before 2001 (no RO data) or after 2001 (RO data are used as calibration references).

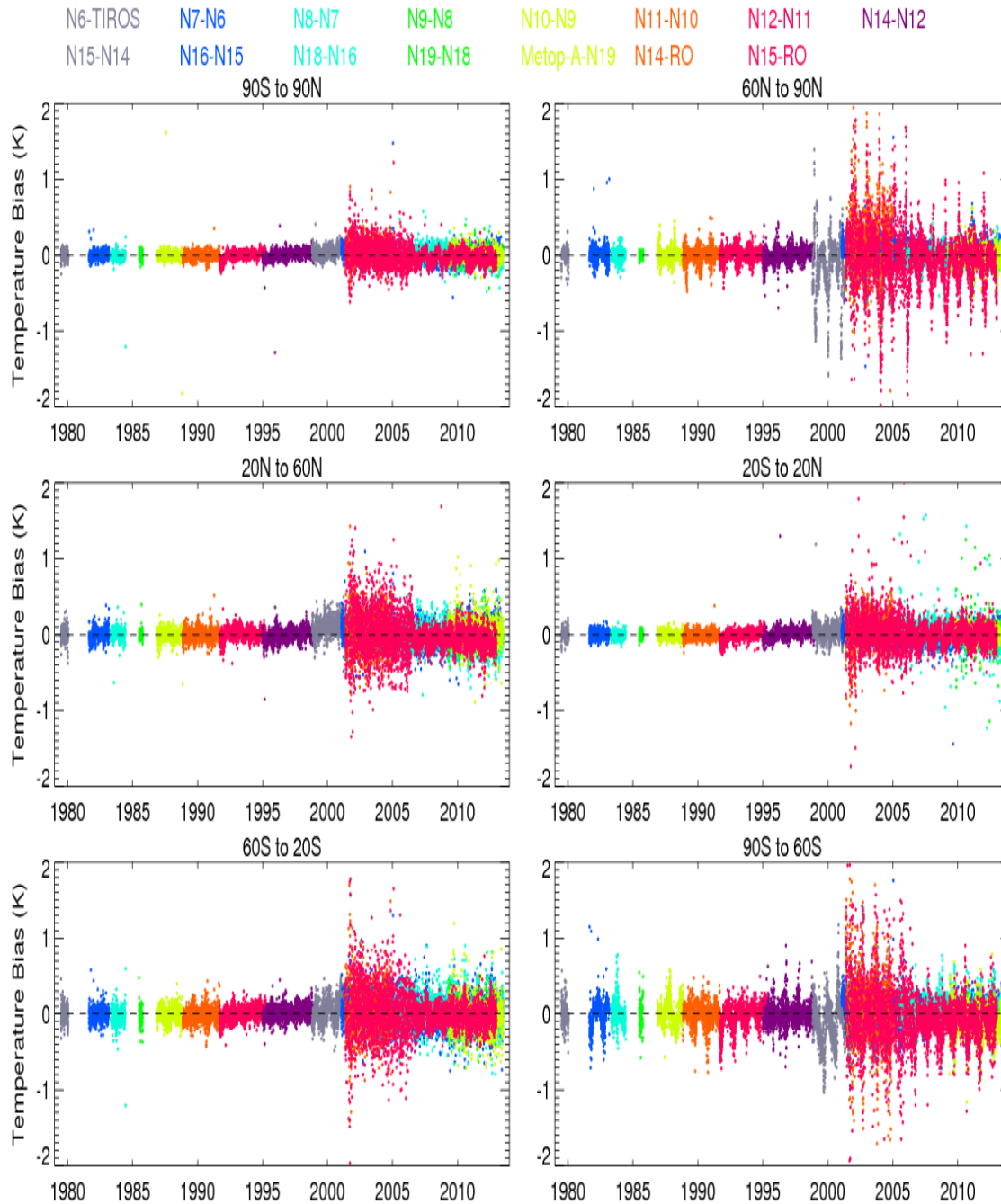


**Figure 10: The time series of the calibrated monthly TLS mean differences for TIROS-N6, N6-N7, N7-N8, N8-N9, N10-N11, N11-N12, N12-N14, N14-N15, N16-N15, N19-N18, N14-RO, N15-RO, and Metop-A-N19 for (a) the entire globe (90°N to 90°S), (b) the 90°N to 60°N zone, (c) the 20°N to 60°N zone, (d) the 20°S to 20°N zone, (e) the 60°S to 20°S zone, and (f) the 90°S to 60°S zone.**

## **5.6 Processing Environment and Resources**

IDL version 7.1 was used to process the data on a x86\_64 server running the CentOS operating system. The ASCII temporary data files require about 7Gb of disk space per month.

## **6. Assumptions and Limitations**

The algorithm assumes that there are a sufficient number of coincident measurements during each month to provide a statistically reliable estimate of slope and offset values.

### **6.1 Algorithm Performance**

N/A

### **6.2 Sensor Performance**

N/A

## **7. Future Enhancements**

### **7.1.1 Enhancement 1 – Revise AQUA Scan Angle Processing**

For version 1.0 results, the AQUA orbiter was processed allowing only scan angles from -10 to +10 degrees. Though the impact on results is small, for version 1.1 the same scan angle range will be used for all orbiters.

### **7.1.2 Enhancement 2 – Improve Algorithm Usage**

To avoid processing errors which result from the user having to edit and re-run programs for different GPSRO missions, polar orbiters, time intervals, etc., The algorithm should be restructured to utilize a single configuration file containing RUN parameters used by all of the processing programs. A single processing program should then implement the algorithm by calling each of the current processing programs as subroutines.

Programs should be restructured so that separate processing of AQUA is eliminated.

Intermediate data file should be stored in a more robust format which does not use so much disk space.

## 8. References

- Anthes, R. A., and Coauthors (2008), The COSMIC/FORMOSAT-3 Mission: Early Results. *Bul. Amer. Meteor. Soc.*, 89(3), 313-333.
- Bean, B.R., E. J., Dutton (1966), Radio Meteorology; National Bureau of Standards Monogr. 92; US Government Printing Office: Washington, DC, USA, 1966.
- Christy, J. R., R. W. Spencer, and W. D. Braswell (2000), MSU Tropospheric temperatures: Data set construction and radiosonde comparisons, *J. Atmos. Oceanic Tech.*, **17**, 1153–1170.
- Christy, J. R., R. W. Spencer, W. B. Norris, W. D. Braswell, and D. E. Parker (2003), Error estimates of Version 5.0 of MSU/AMSU bulk atmospheric temperatures. *J. Atmos. Oceanic Technol.*, **20**, 613–629.
- Christy, J. R., and W. B. Norris (2004), What may we conclude about global tropospheric temperature trends? *Geophys. Res. Lett.*, **31**, L06211, doi:10.1029/2003GL019361.
- Foelsche, U., B. Pirscher, M. Borsche, G. Kirchengast, and J. Wickert (2009), Assessing the Climate Monitoring Utility of Radio Occultation Data: From CHAMP to FORMOSAT-3/COSMIC. *Terr. Atmos. Oceanic Sci.*, **20**, 155-170.
- GCOS (2004), GCOS-92: Implementation Plan for the Global Observing System for Climate in Support of the UNFCCC. WMO/TD, No. 1219, 153pp.
- Grody, N. C., K. Y. Vinnikov, M. D. Goldberg, J. Sullivan, and J. D. Tarpley, Calibration of Multi-satellites observations for climate studies (2004), Microwave Sounding Unit (MSU), *J. Geophys. Res.*, **109**, doi:10.1029/2004JD005079.
- Hajj, G. A., and Coauthors (2004), CHAMP and SAC-C atmospheric occultation results and intercomparisons. *J. Geophys. Res.*, **109**, D06109, doi:10.1029/2003JD003909.
- He, W., S. Ho, H. Chen, X. Zhou, D. Hunt, and Y. Kuo (2009), Assessment of radiosonde temperature measurements in the upper troposphere and lower stratosphere using COSMIC radio occultation data, *Geophys. Res. Lett.*, **36**, L17807, doi:10.1029/2009GL038712.
- Ho, S.-P., Y. H. Kuo, Zhen Zeng and Thomas Peterson (2007), A Comparison of Lower Stratosphere Temperature from Microwave Measurements with CHAMP GPS RO Data, *Geophys. Research Letters*, **34**, L15701, doi:10.1029/2007GL030202.
- Ho, S.-P., M. Goldberg, Y.-H. Kuo, C.-Z Zou, W. Schreiner (2009a), Calibration of Temperature in the Lower Stratosphere from Microwave Measurements using COSMIC Radio Occultation Data: Preliminary Results, *Terr. Atmos. Oceanic Sci.*, Vol. **20**, doi: 10.3319/TAO.2007.12.06.01(F3C).
- Ho, S.-P., G. Kirchengast, S. Leroy, J. Wickert, A. J. Mannucci, A. K. Steiner, D. Hunt, W. Schreiner, S. Sokolovskiy, C. O. Ao, M. Borsche, A. von Engeln, U. Foelsche, S. Heise, B. Iijima, Y.-H. Kuo, R. Kursinski, B. Pirscher, M. Ringer, C. Rocken, and T. Schmidt (2009b), Estimating the Uncertainty of using GPS Radio Occultation Data for Climate Monitoring: Inter-comparison of CHAMP Refractivity Climate Records 2002-2006 from Different Data Centers, *J. Geophys. Res.*, doi:10.1029/2009JD011969.
- Ho, S.-P., W. He, and Y.-H. Kuo (2009c), Construction of consistent temperature records in the lower stratosphere using Global Positioning System radio occultation

- data and microwave sounding measurements, in *New Horizons in Occultation Research*, edited by A. K. Steiner et al., pp. 207–217, Springer, Berlin, doi:10.1007/978-3-642-00321-9\_17.
- Ho, S.-P., Y. H. Kuo, W. Schreiner, X. Zhou (2010) Using SI-traceable Global Positioning System Radio Occultation Measurements for Climate Monitoring [In “States of the Climate in 2009”]. *Bul. Amer. Meteor. Sci.*, in press.
- Kuo, Y. H., T. K. Wee, S. Sokolovskiy, C. Rocken, W. Schreiner, D. Hunt, 2004: Inversion and Error Estimation of GPS Radio Occultation Data. *J. of the Meteor. Society of Japan*, 82(1B), 507-531.
- Mears, C. A., M. C. Schabel, and F. J. Wentz (2003), A reanalysis of the MSU channel 2 tropospheric temperature record, *J. Climate*, 16, 3650–3664.
- Mo. T., M. D. Goldberg, D. S. Crosby, and Z. Cheng (2001), Recalibration of the NOAA Microwave Sounding Unit, *J. Geophys. Res.*, **106**, 10145-10150.
- National Research Council, Committee on Earth Science and Applications from Space: A Community Assessment and Strategy for the Future (2007), *Earth Science and Application from Space: National Imperatives for the Next Decade and Beyond*, National Academies Press, 2007, 456 pp.
- Ohring, G., Ed., (2007), *Achieving Satellite Instrument Calibration for Climate Change*. National Oceanographic and Atmospheric Administration, 144 pp.
- Vinnikov, K. Y., and N. C. Grody (2003), Global Warming Trend of Mean Tropospheric Temperature Observed by Satellites, *Science*, **302**, 269-272.
- Vinnikov, K. Y., N. Grody, A. Robock, R. J. Stouffer, P. D. Jones, and M. D. Goldberg (2006), Temperature Trends at The Surface and in The Troposphere, *J. Geophys. Res.* **111**, D03106, doi:10.1029/2005JD006392, 1-14.
- Ware, R., and Coauthors (1996), GPS sounding of the atmosphere from low Earth orbit: Preliminary results. *Bull. Amer. Meteor. Soc.*, **77**, 19–40.
- WMO, 2007: Final Report for Workshop on the Redesign and Optimization of the Space-based Global Observing System. WMO Headquarters, Geneva.
- Woolf, H., P. van Delst, W. Zhang (1999), NOAA-15 HIRS/3 and AMSU Transmittance Model Validation. Technical Proceedings of the International ATOVS Study Conference, 10th, Boulder, CO, 27 January-2 February 1999. Bureau of Meteorology Research Centre, Melbourne, Australia, 1999, pp.564-573.
- Zou, C. Z., M. Goldberg, Z. Cheng, N. Gordy, J. Sullivan, C. Cao, and D. Tarpley (2006), Recalibration of microwave sounding unit for climate studies using simultaneous nadir overpass. *J. Geophys. Res.* **111**, D19114, doi:10.1029/2005JD006798.
- Zou, C.-Z., M. Gao, and M. Goldberg (2009), Error structure and atmospheric temperature trends in observations from the Microwave Sounding Unit, *J. Clim.*, **22**, 1661–1681, doi:10.1175/2008JCLI2233.1.

## Appendix A. Acronyms and Abbreviations

Acronym or Abbreviation	Meaning
AMSU	Advanced Microwave Sounder Unit
Auqa	Aqua (EOS PM-1) is a multi-national NASA scientific research satellite in orbit around the Earth
CATBD	Climate Algorithm Theoretical Basis Document
CDR	Climate Data Record
CHAMP	Challenging Mini-satellite Payload
CIMSS	Cooperative Institute for Meteorological Satellite Studies
COSMIC	Constellation Observing System for Meteorology, Ionosphere, and Climate
GCOS	Global Climate Observing System
GPS	Global Positioning System
GRACE	Gravity Recovery And Climate Experiment
IDL	Interface description language. This is a specification language used to describe a software component's interface
LECT	Local equator crossing times
LEO	low-Earth orbiting
MERRA	Modern-ERA Retrospective analysis for Research and Applications
MetOP-A	METEorological Operational satellite-A
MSU	Microwave Sounding Unit
MWF	Microwave Forward Model
NASA	National Aeronautics and Space Administration
NCDC	National Climatic Data Center
NESDIS	National Environmental Satellite, Data, and Information Service
NOAA	National Oceanic and Atmospheric Administration
NRC	National Science Council
RO	Radio Occultation
RSS	Remote Sensing System Inc.
SI	System of Units

SNO	Simultaneous Nadir Overpass
SSEC	Space Science Engineer Center
STAR	Center for Satellite Applications and Research
Tb	Brightness Temperatures
TLS	Temperatures in the Lower Stratosphere
UAH	University of Alabama in Huntsville
SSEC	Space Science Engineer Center
STAR	Center for Satellite Applications and Research
Tb	Brightness Temperatures
TLS	Temperatures in the Lower Stratosphere
TTS	Temperatures of Troposphere / Stratosphere
UAH	University of Alabama in Huntsville